Theoretical and experimental spectroscopical study of solvation dynamics

ARTICLE *in* JOURNAL OF MOLECULAR LIQUIDS · AUGUST 1995

Impact Factor: 2.52 · DOI: 10.1016/0167-7322(95)92826-W

2 AUTHORS, INCLUDING:

Boris D. Fainberg
Holon Institute of Technology
104 PUBLICATIONS **527** CITATIONS

ELSEVIER

Journal of Molecular Liquids 64 (1995) 123 – 149

journal of MOLECULAR LIQUIDS

Theoretical and Experimental Spectroscopical Study of Solvation Dynamics

Boris D. Fainberg and Dan Huppert
Raymond and Beverly Sackler Faculty of Exact Science, School of Chemistry, Tel-Aviv University, Ramat Aviv, Tel Aviv 69978, Israel
Received 15 January 1995; accepted 10 May 1995

Abstract

We developed theoretically and experimentally the principles of a spectroscopical method based on resonance transient population gratings for quantitative description of solvation dynamics of large molecules in liquid solutions. The solvation dynamics of LDS 750 in N -monosubstituted amide, ethylacetamide and butylacetamide have been measured. This class of solvents exhibits exceptionally large static dielectric constants. The solvation dynamics of LDS 750 in all solvents consists of ultrafast as well as slow components.

A theoretical basis for solvation dynamics study of complex molecules in solutions by resonance nonlinear spectroscopy has been developed. We have introduced a model of an optically active non-Markovian oscillator (NMO) for the description of solvation dynamics in nonlinear optical experiments in a systematic way. It has been shown that an optically active Brownian oscillator and different NMO models can be considered as successive long time approximations to a real correlation function of an optically active oscillator. The model of two NMOs with an exponential memory function describes accurately various experimental and computer simulations data of ultrafast solvation dynamics. We have compared the latter model with modern theories of solvation.

1. Introduction

Ultrafast time-resolved spectroscopy has been applied to probe the dynamics of electronic spectra of molecules in solutions [1-5]. Typically, a fluorescent probe molecule is electronically excited and the fluorescence spectrum is monitored as a function of time. Relaxation of the solvent polarization around the newly created excited molecule state led to a time dependent Stokes shift of the luminescence spectrum. Such investigations are aimed to study the mechanism of solvation effects on electron transfer processes, proton transfer, etc. [1-5].

In recent ultrafast experiments the fast (subpicosecond) components in the solvation process have been observed [4-5]. Transient resonance degenerate four-wave mixing has been used for the observation of ultrafast solvation dynamics [6-8] (see also references 9-10). In this method (figure 1), two short pump pulses with wave vectors $\mathbf{k}_1$ and $\mathbf{k}_2$ create a light-induced grating in the sample under investigation with a wave vector $\mathbf{q} = \mathbf{k}_1 - \mathbf{k}_2$. The grating effectiveness is measured by the diffraction of a time delayed probe pulse $\mathbf{k}_3$ with the generation of a signal with a new wave vector $\mathbf{k}_s = \mathbf{k}_3 + (\mathbf{k}_1 - \mathbf{k}_2)$. This method is characterized by a high time resolution and provides additional spectroscopical information, in particular it senses the dynamics in the ground electronic state which is principally absent in luminescence measurements.

One must distinguish between the transient resonance degenerate four-wave mixing

experiments with very short pump pulses [6,9-10] $t_p \sim 10$ fs from the experiments with relatively long pulses with $t_p \sim 150$ fs (see this work and [7-8]). The experimental conditions of our transient degenerate four-wave mixing experiments have been designed to provide similar information to the ones given by time-resolved luminescence (TRL)studies. TRL experiments investigate the hot luminescence processes occurring after the completion of the electronic transition phase relaxation (with a characteristic decay time T′) and during the vibrational and solute-solvent relaxation in the excited electronic state. Therefore, we conducted our resonance four- wave mixing experiments [7-8] in such a way to prevent the polarization gratings and to preserve the population gratings. The polarization gratings are destroyed during the phase relaxation time T′ of the electronic transition, and the population ones are destroyed during the vibrational relaxation time τ_c.

We shall consider molecules with broad structureless (or weakly structured) electronic spectra for which the following inequality is fulfilled:

$$\sigma_2 \tau_c^2 >> 1 \tag{1}$$

where σ_2 is the second central moment of an electronic spectrum. It has been demonstrated that the following times are typical for the time evolution of the system investigated [11-15]:

$$\sigma_2^{-1/2} < T' << \tau_c \tag{2}$$

where $\sigma_2^{-1/2}$ plays the role of the reversible dephasing time of an electronic transition, $T' = (\tau_c \sigma_2^{-1})^{1/3}$ plays the role of the irreversible dephasing time, and τ_c plays the role of the relaxation time of populations. The typical value of the irreversible dephasing time for complex molecules in solutions for usual conditions $T' \approx 20$ fs [11]. Therefore, the character of the response of the system under study ($\sigma_2 \tau_c^2 >> 1$) in degenerate four-wave mixing experiment depends on the relation between T′ and the pump pulses

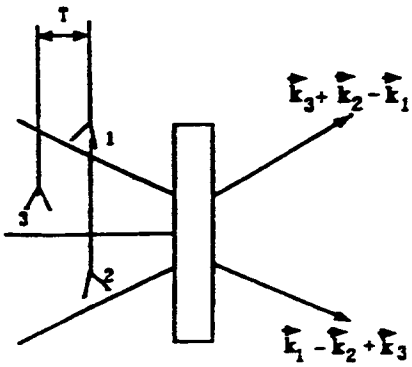

Fig. 1. Geometry for transient grating spectroscopy.

duration t_p [11-12].

In our experiments the pump pulse duration $t_p >> T'$ (t_p ~150 fs). Relatively long pump pulses $t_p >> T'$ of frequency ω create a hole in the initial thermal distribution relative to a generalized solvation coordinates in the ground electronic state (Fig. 2) and, simultaneously, a narrow spike in the excited electronic state. These changes are measured by the probe pulse at the same frequency ω. In the next sections we shall term degenerate four wave mixing spectroscopy with long pump pulses $t_p >> T'$ as resonant transient population grating spectroscopy (RTPGS).

In recent papers [7-8] we have reported on solvation dynamics studies using RTPGS. The solvation dynamics of LDS 750 dye in alkanols like metanol, ethanol, propanol and in diols 1,2-ethanediol, 1,3-propanediol and 1,4-butanediol have been measured. In this study we extended our previous RTPGS measurements to a new class of associative liquids - the N-monosubstituted amides. This class of solvents exhibit exeptionally large static dielectric constants.

We have previously developed the theory of the RTPGS for solvation dynamics study using the approach of four-time correlation functions and obtained expressions for the case when the perturbation of the molecular nuclear system during the electronic transition is a Gaussian quantity [7-8,16]. In particular, the latter reduces to the mirror symmetry of the equilibrium absorption and luminescence spectra. However, the absorption and luminescence spectra of the molecule LDS 750, used in our experiments, do not satisfy to the law of the mirror symmetry. Therefore, in Ref.17 we have developed another approach to calculate the RTPGS signal. We took into account the conditions (1)-(2), and also $t_p >> T' \equiv (\tau_c \sigma_2^{-1})^{1/3}$ ab initio. Such an approach allows us to solve concrete problems, in particular, to generalize the theory [7-8,16] for the case of

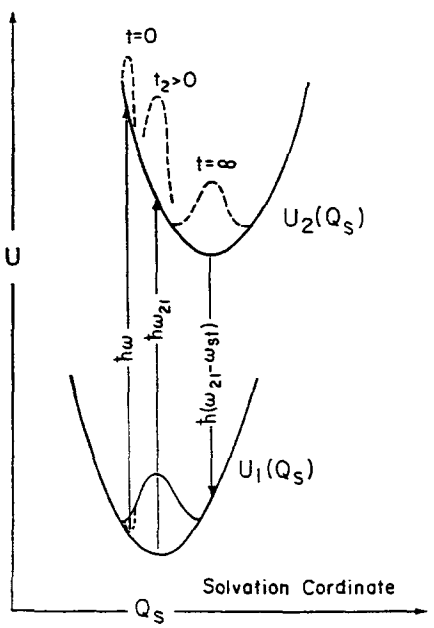

Fig. 2. Potential surfaces of the ground and the excited electronic states of a solute molecule in liquid. One dimensional potential surfaces as a function of a generalized solvent polarization coordinate.

arbitrary shapes of the intramolecular spectra (non-Gaussian case). Here it will be used for modelling the RTPGSsignal from the molecule LDS 750.

Furthermore, theories [7-8,16] and also the theory presented in this paper, connect the nonlinear optical response of a molecule in a solution with the correlation function S(t) that describes solvation dynamics (see below). The analytical form of S(t) can be arbitrary in principal. Its calculation is an independent problem.

For the aim of the description of linear and nonlinear response, a model which should be described by a simple enough correlation function S(t), is needed, in order to obtain results which can be treated, to achieve a comparison with an experiment. On the other hand, such a model must be sufficiently real. In this regard, recently stochastic models were studied on a large scale [5-6,9-19] . The model of an optically active Brownian oscillator (BO) became very popular in linear absorption [20], Raman scattering [21], four-photon [6,22-25], and time resolved luminescence [5] spectroscopy. Yan and Mukamel have introduced this model for an optical response by a systematic way [23]. The popularity of the optically active BO model is due to the very simple analytical form of its correlation function. Such a model was broadly used in spite of the fact that its correctness criteria [21] is often not fulfilled [26]. In contrast we have proposed [26] a model of an optically active non-Markovian oscillator (NMO). Here we introduce a model of an optically active NMO by a systematic way. We show that an optically active BO and different NMO models can be considered as successive long time approximations to a real correlation function of an optically active oscillator. We obtain simple expressions for the relaxation and correlation functions of an NMO with an exponential memory function, and apply them to the description of solvation dynamics of a probe molecule.

It is worth noting that the concept of an optically active NMO exceeds the limits of being able to describe only the solvation dynamics. It is also interesting from the point of view of a general description of vibronic transitions in linear and nonlinear optical experiments.

2. Theoretical background

Let us consider a molecule with two electronic states n=1 and 2 in a solvent described by the Hamiltonian

$$H_0 = \sum_{n=1}^{2} |n\rangle \left[E_n - i\hbar\gamma_n + W_n(Q)\right] \langle n|, \; E_2 > E_1 \tag{3}$$

where E_n and $2\gamma_n$ are the energy and inverse lifetime of state n, $W_n(Q)$ is the adiabatic Hamiltonian of a reservoir R(the vibrational subsystems of a molecule and a solvent interacting with the two-level electron system under consideration in state n).

The molecule is affected by electromagnetic radiation of three beams

$$\mathbf{E}(\mathbf{r},t) = \mathbf{E}^{+}(\mathbf{r},t) + \mathbf{E}^{-}(\mathbf{r},t) = \frac{1}{2} \vec{\mathcal{E}}(\mathbf{r},t) \exp(-i\omega t) + \text{c.c.},$$

where $\vec{\mathcal{E}}(\mathbf{r},t) = \sum_{m=1}^{3} \vec{\mathcal{E}}_m(t) \exp(i\mathbf{k}_m \mathbf{r})$.

Since we are interested in the solvent-solute intermolecular relaxation, we shall single out the solvent contributions to E_n and $W_n(Q)$,

$$E_n = E_n^o + \langle V_n^{el} \rangle, \tag{4}$$

$$W_n(Q) = W_{nM} + W_{ns}, \quad W_{ns} = W_{so} + \bar{W}_{ns} \tag{5}$$

where W_{so} is the Hamiltonian governing the nuclear degrees of freedom of the solvent in the absence of the solute, W_{nM} is the Hamiltonian representing the nuclear degrees of

freedom of solute molecule, E_n^o is the energy of state n of the isolated molecule, $\bar{W}_{ns}$ and V_n^{el} describe interactions between the solute and the nuclear and electronic degrees of freedom of the solvent, respectively. It is possible to replace the operators V_n^{el} in the Hamiltonian by their expectation values $\langle V_n^{el} \rangle$ [27].

A signal in any method of four-photon spectroscopy can be expressed by nonlinear polarization $\mathbf{P}^{NL}$. The signal power I_s in the $\mathbf{k}_s$ direction at time t is proportional to the square of the modulus of the corresponding component of the cubic polarization $\mathbf{P}^{(3)+}$:

$$I_s(t) \sim |\mathbf{P}^{(3)+}(\mathbf{r},t)|^2 \tag{6}$$

In pulsed experiments one usually measures the dependence of the signal energy J_s on the delay time τ of the probe pulse relative to pump ones:

$$J_s(\tau) \sim \int_{-\infty}^{\infty} dt \; |\mathbf{P}^{(3)+}(\mathbf{r},t)|^2 \tag{7}$$

Our main interest is in the solvation dynamics irrespective of the behavior of the molecule. Numerous experiments [28-30] show that a Franck-Condon molecular state, achieved by an optical excitation, relaxes very fast, and the intramolecular spectra form within 0.1 ps (concerning the interpretation of experiments [28] see Ref. 31). Therefore, we shall consider that in our experiments the intramolecular relaxation takes place within the pulse duration ($t_p \approx 150$ ps). More exactly, there are fast and slow steps in the relaxation of a Franck-Condon state: the faster component is mainly determined by the intramolecular relaxation while the slower step is determined by the intermolecular relaxation. For these conditions, one can consider that a molecule is in the equilibrium state characterized by the equilibrium density matrix $\rho_{kM} = \exp(-\beta W_{kM})/Tr_{R_M} \exp(-\beta W_{kM})$, where k=1,2; $\beta=1/kT$ and Tr_{R_M} denotes the operation of taking track with respect to the molecular degrees of freedom.

We shall calculate $\mathbf{P}^{(3)+}(\mathbf{r},t)$, using a general theory [17]. For the conditions under consideration, the formula for the positive frequency component of the resonance polarization takes the following form [17]:

$$\mathbf{P}^{+}(\mathbf{r},t) = \frac{\pi}{2\hbar} N \mathbf{D}_{12}\left(\mathbf{D}_{21} \vec{\mathcal{E}}(\mathbf{r},t)\right) \left\{ i\left[F_\alpha(\omega,\omega,t) - F_\varphi(\omega,\omega,t)\right] + \left[\Phi_\alpha(\omega,\omega,t) - \Phi_\varphi(\omega,\omega,t)\right] \right\} \tag{8}$$

where N is the density of solute molecules, $\mathbf{D}_{12}$ is a matrix element of the dipole-moment operator taken with respect to the electron wave functions,

$$F_{\alpha,\varphi}(\omega_1,\omega,t) = \int_{-\infty}^{\infty} d\omega' \; F_{\alpha,\varphi_M}(\omega') \; F_{\alpha,\varphi_S}(\omega_1 - \omega_{el} - \omega',\omega,t) \tag{9}$$

are the spectra of the non-equilibrium absorption (α) or luminescence (φ) of a molecule in solution, $\omega_{el} = (E_2 - E_1)/\hbar$ is the frequency of the pure-electronic transition $1 \rightleftarrows 2$, $F_{\alpha,\varphi_S}(\omega',\omega,t)$ and

$$F_{\alpha,\varphi_M}(\omega') = \frac{1}{2\pi} \int_{-\infty}^{\infty} d\tau_1 \; Tr_{R_M}\left[\exp(\pm i/\hbar \; W_{2,1M}\tau_1) \exp(\mp i/\hbar \; W_{1,2M}\tau_1) \; \rho_{1,2M}\right] \exp(-i\omega'\tau_1) \tag{10}$$

are the corresponding "intermolecular" (s) and "intramolecular" (M) spectra;

$$\Phi_{\alpha,\varphi}(\omega_1,\omega,t) = \frac{P}{\pi}\int_{-\infty}^{\infty} d\omega' \frac{F_{\alpha,\varphi}(\omega',\omega,t)}{\omega'-\omega_1} \qquad (11)$$

are the non-equilibrium spectra of the refraction index which are connected with the corresponding spectra $F_{\alpha,\varphi}(\omega_1,\omega,t)$ by the Kramers-Kronig formula, P is the symbol of the principal meaning.

"Intermolecular" spectra $F_{\alpha,\varphi s}(\omega',\omega,t)$ are determined by the solvent contribution (due to the fact that the quantities of the type of $u_S = W_{2S} - W_{1S} \neq 0$) to the electronic spectra. In the four-photon approximation they can be written by Eq.(14) (see below).

Let us limit ourselves by the Gaussian value u_S. The Gaussian approximation is valid for the description of the intermolecular relaxation [27,32]. The interaction energy of the solute molecule with its surroundings can be represented as the sum of the energy of interaction with the individual solvent molecules. Accordingly, the quantity $u_S(t)$ can be also represented as a sum $u_S(t) = \sum_j u_{Sj}(t)$ of random variables $u_{Sj}(t)$ associated with jth solvent molecule, correspondingly. The number of such solvent molecules (j) can be quite large (in the absence of specific chemical interactions). In addition, the contributions $u_{Sj}(t)$ can be considered for a liquid as weakly correlated. According to the central limit theorem of the probability theory [33], these properties of $u_{Sj}(t)$ permit one to consider the magnitude $u_S(t)$ as a Gaussian stochastic function [32].

Using the Gaussian and four photon approximations, we can obtain the following expression for the spectra $F_{\alpha,\varphi}(\omega_1,\omega,t)$ [17]:

$$F_{\alpha,\varphi}(\omega_1,\omega,t) = \mp \frac{\pi}{2\hbar^2}\int_0^t d\tau_2 \,|\mathbf{D}_{21}\,\vec{\mathcal{E}}(\mathbf{r},t-\tau_2)|^2 \iint_{-\infty}^{\infty} d\omega' d\omega'' \, F_{\alpha M}(\omega') \cdot F^e_{\alpha S}(\omega-\tilde{\omega}_{21}-\omega') \cdot$$
$$\cdot F_{\alpha,\varphi M}(\omega'') \;\; F_{\alpha,\varphi s}(\omega_1-\omega_{\alpha,\varphi},\tau_2) \qquad (12)$$

$$\Phi_{\alpha,\varphi}(\omega_1,\omega,t) = \pm \frac{\sqrt{\pi}}{\hbar^2}\int_0^t d\tau_2 \,|\mathbf{D}_{21}\,\vec{\mathcal{E}}(\mathbf{r},t-\tau_2)|^2 \iint_{-\infty}^{\infty} d\omega' d\omega'' \, F_{\alpha M}(\omega') \cdot F^e_{\alpha S}(\omega-\tilde{\omega}_{21}-\omega') \cdot$$
$$\cdot F_{\alpha,\varphi M}(\omega'') \;\; X_{\alpha,\varphi s}(\omega_1-\omega_{\alpha,\varphi},\tau_2) \qquad (13)$$

where

$$F_{\alpha,\varphi s}(\omega_1-\omega_{\alpha,\varphi},\tau_2) = (2\pi\sigma(\tau_2))^{-1/2} \exp\left\{ -\frac{[\omega_1-\omega_{\alpha,\varphi}(\tau_2)]^2}{2\sigma(\tau_2)} \right\} \qquad (14)$$

are the changes related to non-equilibrium solvation processes in the absorption (F_α) and the emission (F_φ) spectra,

$$X_{\alpha,\varphi s}(\omega_1-\omega_{\alpha,\varphi},\tau_2) = F_{\alpha,\varphi s}(\omega_1-\omega_{\alpha,\varphi},\tau_2)\,\mathrm{Erfi}\left[(\omega-\omega_{\alpha,\varphi}(\tau))/(2\sigma(\tau_2))^{1/2}\right] \qquad (15)$$

are the changes related to non-equilibrium solvation processes in the refraction index,

$\mathrm{Erfi}(x) = \int_0^x \exp(y^2)\,dy$,

$$\omega_{\alpha,\varphi}(\tau_2) = \tilde{\omega}_{21} + \omega'' + (\omega-\tilde{\omega}_{21}-\omega')\,\mathrm{ReS}(\tau_2) - \delta_{(\alpha,\varphi)\varphi} 2\sigma_{2S}\cdot \mathrm{Im}\int_0^{\tau_2} S(x)\,dx, \qquad (16)$$

$\delta_{(\alpha,\varphi)\varphi}$ is the Kronecker symbol ($\delta_{(\alpha,\varphi)\varphi} = \delta_{\alpha\varphi} = 0$ for $\omega_\alpha(\tau_2)$ and $\delta_{(\alpha,\varphi)\varphi} = \delta_{\varphi\varphi} = 1$ for $\omega_\varphi(\tau_2)$), $\bar{\omega}_{21} = \omega_{el} + \omega_{St}/2$, $\omega_{St} = 2\,\mathrm{Tr}\,(u_S \rho^e_{1S}) \equiv 2\langle u_S\rangle$ is the solvent contribution to the Stokes shift between the equilibrium absorption and emission spectra, ρ^e_{1S} denotes the equilibrium density matrix of a solvent, $\hbar^2\sigma_{2S}S(t) = \langle u_S(0)u_S(t)\rangle - \langle u_S\rangle^2$, S(t) is the normalized solute-solvent correlation function, $\sigma_{2S} = \hbar^{-2}(\langle u_S^2(0)\rangle - \langle u_S\rangle^2)$ is the contribution of the solvent to the second central moment of both the absorption and the luminescence spectra, $u_S(t) = \exp((i/\hbar)W_1 t)\, u_S \exp((-i/\hbar)W_1 t)$,

$$\sigma(\tau_2) = \sigma_{2S}(1 - \mathrm{Re}^2 S(\tau_2)) \tag{17}$$

is the time dependent second central moment,

$$F^e_{\alpha S}(\omega-\omega_1) = (2\pi\sigma_{2S})^{-1/2} \exp\left[-(\omega-\omega_1)^2/2\sigma_{2S}\right] \tag{18}$$

is the equilibrium solvent contribution to the absorption spectrum. We do not limit our consideration here by the classical (high-temperature) approximation for the solvation dynamics. Let us consider this issue in more detail. In the general (quantum) case, the correlation function S(t) is complex and it is not an observable quantity. Therefore, it is difficult to treat its physical meaning. It is more convenient to deal with the relaxation function $\Phi_r(t)$ which describes the relaxation of a system after removal of the external disturbance [34]. Unlike the correlation function, $\Phi_r(t)$ is always a real observable function.

Let us introduce the Fourier transforms of $\sigma_{2S}S(t)$ and $\Phi_r(t)$:

$$\begin{bmatrix} s(\omega) \\ \phi(\omega) \end{bmatrix} = \frac{1}{2\pi}\int_{-\infty}^{\infty} dt\, \exp(-i\omega t) \begin{bmatrix} \hbar^2\sigma_{2S}S(t) \\ \Phi_r(t) \end{bmatrix} \tag{19}$$

$s(\omega)$ and $\phi(\omega)$ satisfy the following relation [34-35]:

$$s(\omega) = \left\{\hbar\omega/\left[1-\exp(-\hbar\omega\beta)\right]\right\}\phi(\omega) \tag{20}$$

Using the inverse Fourier transformation, we obtain from Eq. (20):

$$S(t) = \frac{1}{2\hbar\sigma_{2S}}\left[2\int_0^{\infty} \omega \coth\frac{\hbar\omega\beta}{2}\,\phi(\omega)\cos\omega t\, d\omega - i\frac{d\Phi_r}{dt}\right] \tag{21}$$

The latter allows one to find the correlation function if the relaxation function is known[1]. Using Eq. (21), we obtain the following expression for the time dependent frequency of the nonequilibrium emission spectrum

$$\omega_\varphi(\tau_2) = \bar{\omega}_{21} + \omega'' + (\omega - \bar{\omega}_{21} - \omega')\,\mathrm{Re}S(\tau_2) - \hbar^{-1}\Phi_r(0)\left[1 - f_r(\tau_2)\right] \tag{22}$$

where $f_r(t) = \Phi_r(t)/\Phi_r(0)$ is the normalized relaxation function. For the classical limit ($\hbar\omega\beta \ll 1$) $\hbar^2\sigma_{2S}\mathrm{Re}S(\tau_2) = \beta^{-1}\Phi_r(\tau_2)$, i.e. the normalized real part of the classical correlation function coincides with the $f_r(t)$. In addition, for the classical case

[1] For high-temperature (classical) case ($\hbar\omega\beta \ll 1$) $\phi(\omega) = \beta s_{cl}(\omega)$. The substitution of the latter expression for $\phi(\omega)$ in Eq. (20) reduces to the relation between $s(\omega)$ and $s_{cl}(\omega)$, obtained in a different way [26].

$\sigma_{2S} = \omega_{st}\hbar^{-1}\beta^{-1}$, therefore

$$\Phi_{\Gamma_{cl}}(0) = \hbar\omega_{st} \tag{23}$$

In the last case, Eq. (22) for the frequency $\omega_{\varphi}(\tau_2)$ reduces to the expression we obtained before [7-8,16].

3.Comparison of nonlinear optical spectroscopy with TRL

The TRL signal is determined by the value $F_{\varphi}(\omega_f, \omega, t)$ (Eq.(9)), where ω_f is the radiated frequency, ω is the excitation frequency. One can see the close connection of the TRL spectroscopy with nonlinear optical spectroscopy. The corresponding signals are determined by the nonequilibrium absorption and emission processes. The TRPGS signal is determined by both the non-equilibrium processes of the absorption and emission and also by corresponding refraction index spectra at the frequency ω (see Eqs. (6)-(8)). In contrast to the TRPGS, the TRL signal is determined only by $F_{\varphi}(\omega_f, \omega, t)$, i.e. by the relaxation processes in the excited electronic states. However, in TRL spectroscopy, the whole spectrum is measured while in RTPGS only the excitation frequency is monitored.

It is worthwhile noting that these conclusions have been obtained without using the four-photon and Gaussian approximations.

4.Modeling RTPGS signal

Let us use the developed theory for modeling RTPGS signal. Fig. 3 illustrates the time behavior of the signal $J_S(\tau)$ which was calculated for the limit of short pump pulses by formulae (7), (8), (12)-(18). The shapes of "intramolecular" spectra $F_{\alpha,\varphi_M}(\omega')$ are modeled by the same dependence as that in Refs.[7-8,16], but generalized for the case of non-mirror-symmetric spectra $F_{\varphi_M}(\omega')$ and $F_{\alpha_M}(\omega')$: $F_{\alpha_M}(\omega') \sim \bar{S}^{x_\alpha}/\Gamma(x_\alpha+1)$ where $\Gamma(x+1)$ is the gamma-function, $x_\alpha = (\omega'-\omega_{el})/(4\omega_o/3)$, and $F_{\varphi_M}(\omega') \sim \bar{S}^{-x_\varphi}/\Gamma(-x_\varphi+1)$, $x_\varphi = (\omega'-\omega_{el})/(2\omega_o/3)$. We used the following values for the parameters: $\omega_{st}(2\sigma_{2s})^{-1/2} = 2$, $\bar{S} = 1.5$, $\omega_o(2\sigma_{2s})^{-1/2} = 1.14$. The "intramolecular" spectra $F_{\alpha_M}(\omega')$ and $F_{\varphi_M}(\omega')$ for these parameters are shown in Fig. 4 in the form of the equilibrium spectra $F_{\alpha_M}(\omega-\omega_{el})$ and $F_{\varphi_M}(\omega_{el}-\omega)$ when the contribution from the solvent is absent. The equilibrium spectra of

the molecule in solution $F^{e}_{\alpha}(\omega-\omega_{21})$ and $F^{e}_{\varphi}(\omega_{21}-\omega_{st}-\omega)$ are also shown in Fig.4. The

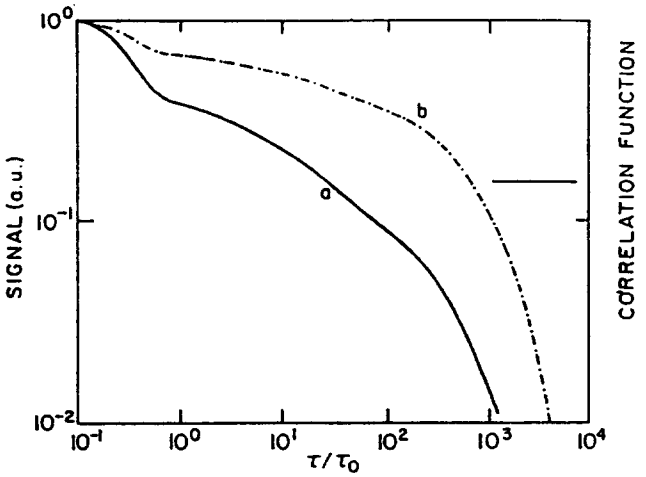

Fig. 3. Model calculations of the RTPGS signal (a); the solvation correlation function (b) consists of a Gaussian followed by three exponential decays (formula (23a)); note the curves are on a logarithmic scale, therefore the constant part of the $J_S(\tau)$ signal has been substracted; τ_0=200 fs, $T_1/\tau_0=\infty$, $a_3\cdot\tau_0^2$=7.7016, $a_1\cdot\tau_0$=0.33, $a_5\cdot\tau_0$=0.04, a_2=0.3, $a_4=a_6=a_8$=0.2, $a_7\cdot\tau_0$=0.00286, $a_9\cdot\tau_0$=0.00074.

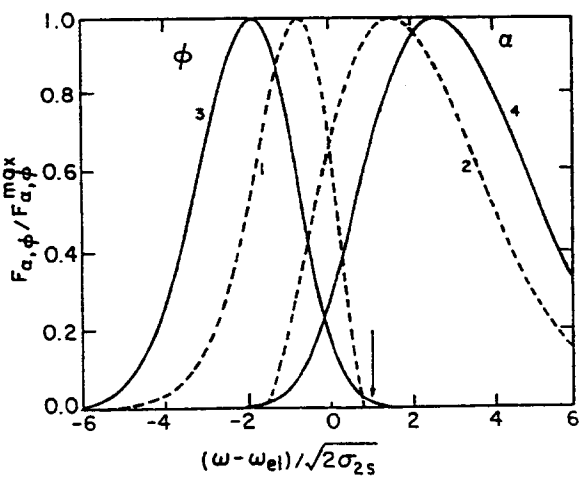

Fig. 4. The shapes of the "intramolecular" spectra $F_{\alpha,\varphi_M}(\omega')$. 1 and 2 are the equilibrium luminescence and absorption spectra of a molecule, respectively, when the solvent contribution from the solvent is absent; 3 and 4 are the equilibrium spectra of a molecule in solution. The arrow shows the relative position of excitation frequency ω for the four-photon signal calculations (Fig.3).

lattersare similar to the absorption and luminescence spectra of the molecule LDS 750 in solution used in our experiments.

It follows from Eqs.(7)-(9), (11)-(16), (22) that the signal $J_S(\tau)$ depends on the excitation frequency ω. We chose $\omega = \omega_{el} + \omega_{st}/2$ which approximately corresponds to the experimental situation. We use here the following form for the correlation function S(t):

$$S(t) = a_2 \exp(-a_3 t^2) + (1-a_2-a_4- a_6-a_8) \exp(-a_1 t)+a_4 \exp(-a_5 t) +a_6 \exp(-a_7 t) + + a_8 \exp(-a_9 t) \quad (23a)$$

The first addend in expression (23a) corresponds to a fast Gaussian component, observed in [4]. The second one corresponds to the relatively fast exponential component with an attenuation time of 200-400 fs observed in [4]and in our experiments. The third component corresponds to a slower attenuation with a decay time of the longitudinal relaxation τ_L. It is worth noting that such a division by different contributions to the correlation function is purely formal, and is used here to impart the realistic form of the correlation function. As a matter of fact, both the short and the long time components of the correlation function are manifestations of one physical process. We shall discuss this issue below. We also showed in Fig.3 the time dependence of the corresponding correlation functions $S(\tau)$, used for the calculation of corresponding signal $J_S(\tau)$.

One can see that the dependencies $S(\tau)$ and $J_S(\tau)$ are very similar (but not identical), and the signal $J_S(\tau)$ reflects the fine details of $S(\tau)$. Fig. 5 shows the experimental RTPGS signal of LDS 750 in 1,3-propanediol [7-8]. One can see that the experimental (Fig. 5) and the theoretical (Fig. 3) behaviours of the signal are similar. Thus, the RTPGS can be used for the ultrafast study of the solvation dynamics.

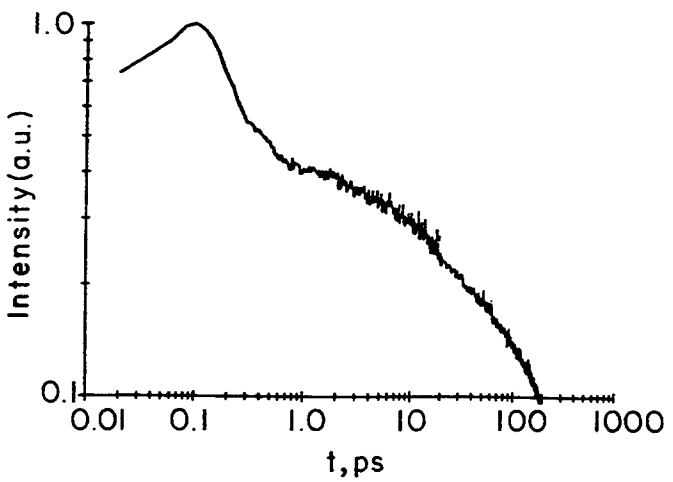

Fig. 5. RTPGS signal of LDS 750 in 1,3-propanediol.

5.Experimental Details

The laser source consists of a CW mode locked amplified dye laser. Detailed experimental description of the system is given in references [7-8]. A small portion of a CW mode locked Nd:YAG 1.06 μm radiation is amplified by a CW Nd:YAG regenerative amplifier operating at 500 Hz. The doubled frequency output of the amplifier was used to amplify the ultrashort dye laser pulse 140 fs FWHM, 1 nJ generated by a synchronously pumped dye laser. A dye amplifier consists of three flowing dye cells was pumped by the regenerative amplifier second-harmonic pulse. The dye laser amplification is achieved by DCM dye to ~15 μJ with a pulse width comparable with the non-amplified pulse.

In the four wave mixing optical setup the laser pulse was split into three beams. Optical delay lines were used to overlap in time the pump beams and to control the time delay of the probe beam. The three beams (parallel polarization) were focused onto the sample by a single lens of 50 cm focal length. In DFWM experiments the signal beam exit the sample at a unique direction $\mathbf{k}_S=(\mathbf{k}_1-\mathbf{k}_2)+\mathbf{k}_3$ and therefore it is easily separated from the three generation beams.

LDS 750 (styryl 7) was purchased from Exciton and was used without further purification. The solvent used were either analytical or of a spectroscopical grade. Samples were circulated in a flowing cell of 1 mm pathlength.

6.Experimental Results

Time-resolved four-wave mixing signals of LDS 750 in ethylacetamide and butylacetamide are shown in Fig.6. The signals were collected with relatively low time resolution by scanning the probe beam delay stage at 0.5 ps time steps. As seen from the figure the signal decay curves for LDS 750 in these solvents are nonexponential and consist of several time domains. The long life time component of LDS 750 in both liquids we attribute to the decay of the electronic population grating. The excited state

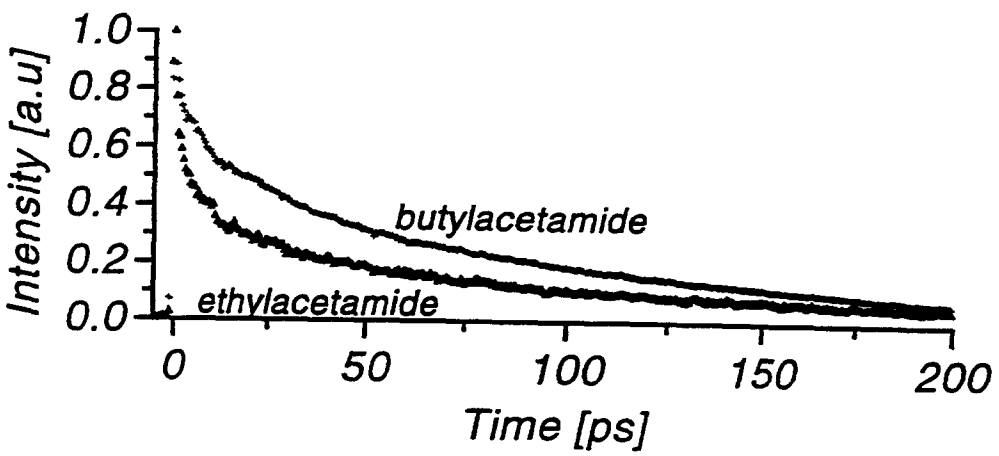

Fig.6. RTPGS signals of LDS 750 in ethylacetamide and butylacetamide solutions.

lifetime of LDS 750 in these liquids is about twice longer than the longest decay

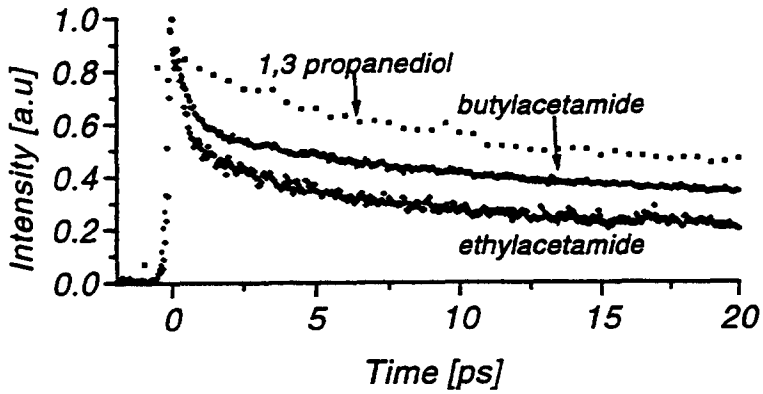

Fig.7. RTPGS signals of LDS 750 in both amides and in 1,3-propanediol solutions.

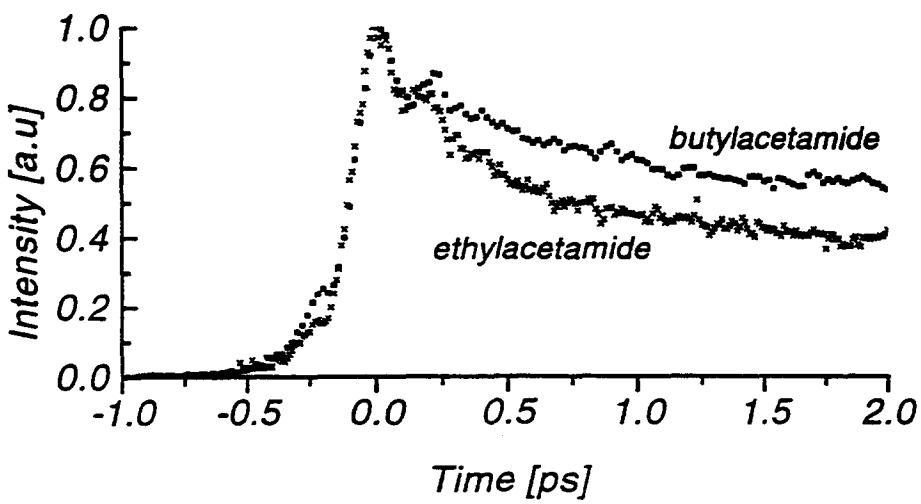

Fig.8. High time resolution signal of the first 2 picoseconds of LDS 750 in ethylacetamide and butylacetamide solutions.

time of the DFWM signals since the DFWM signal is proportional to $|P^{(3)+}|^2$ and $P^{(3)+}$ decays as exp $(-\tau/T_1)$ where T_1 is the excited state lifetime.

The shorter time components of the DFWM signal of LDS in ethylacetamide and butylacetamide are shown in Fig.7. The signals are shown on a time scale of 20 picosecond with 50 fs time steps. Each of the decay curves shown in Fig.7 consists of several time components. All of these time components we attribute to the complex solvation dynamics of LDS 750 in acetamide solvents.

The longest component can be approximately fitted to an exponential decay of 10 and 50 ps for ethyl and butyl acetamide respectively. These relaxation times correspond roughly to the longitudinal dielectric relaxation time τ_L of the particular liquid. The dielectric properties of amides were studied by Bass and Cole [36] and Danhauser and Johari [37].

Leader and Gormley [38] reported in 1951 of the exceptionally large static dielectric constant of liquid N-monosubstituted amides. They suggested that the large dielectric constants of these liquids must be attributed to intermolecular association into essentially linear chain by CO....HN hydrogen bonds. The degree of association is usually given in terms of the dipole correlation factor g of Kirkwood. The size of the amine alkyl group affects the magnitude of the dielectric constant to a greater extent than the size of the acid alkyl group in isomeric amides [39]. It was also found [39] that the size and shape of the alklyl substituent of the amine was of secondary importance to the intermolecular association.

The dielectric relaxation for several amides was measured in the range 0.5-200 MHz [36-37]. The slow relaxation kinetics for the amides appear to be characteristic of hydrogen-bonded liquids (alkyl halides liquid relaxation is about 1200 times faster). Despite the large difference in molecular structure and the extent of intermolecular association as deduced by the Kirkwood correlation factor, the dielectric relaxation in alcohols and amides with similar molecular weight parallels both in magnitude and temperature dependence.

The short time components of the DFWM signals of LDS 750 in ethylacetamide and butylacetamide solution, are shown in Fig.8, using 20 fs time steps of the probe beam delay stage. The DFWM signal of both solvents consists of an ultrashort spike followed by a ~400 fs decay. The initial Gaussian shape spike is caused by a contribution of two superimposed components. A coherent contribution arises due to repumping of energy from the pumping beams to the probe beam and is often found in DFWM experiments. The coherent spike full width half maximum is determined by the laser pulse correlation function and hence by the laser pulse width. The coherent spike prevents us for the time being to resolve accurately the first ~150 fs of the solvation dynamics.

The ultrafast solvation dynamics of LDS 750 in acetonitrile was studied by Rosenthal et al. [4] using time resolved luminescence technique with ~125 fs FWHM instrument response function. The solvation response consisted of two distinctive parts. A fast initial decay accounted for ~ 80% of the amplitude was fit by a Gaussian. The slower tail decayed exponentially with a decay time of 200 fs. In a subsequent study, Cho et al. [5] measured the time dependent non resonant optical Kerr effect in neat acetonitrile liquid. Both experiments have shown the biphasic character of the solvent response. A vibrational model was used to describe quantitatively the solvation and the neat liquid dynamics [5]. A number of Brownian oscillators with frequency distribution of the vibrational modes produce a very good fit of both experimental data.

The shortest time component has a Gaussian shape but can not be time resolved since the coherent spike is superimposed on it. Also the pulse duration in our experiment is longer than the predicted Gaussian component of the solvation. The solvation dynamics on the short time scale < 2 ps of LDS 750 in ethylacetamide and butylacetamide is quite similar. The relative height of the coherent spike superimposed on the Gaussian component versus the subsequent total signal is the same in both liquids. The decay time of the

exponential component is ~400 fs for both liquids, about twice the decay time found in acetonitrile [4]. We now wish to compare the solvation dynamics on the short time scale <2ps of LDS 750 in methanol, and diols, previously studied by us [7-8], with the current measurements of acetamides. On this short time scale the solvation dynamics in methanol, diols and amide is quite similar. The relative height of the coherent spike superimposed on the Gaussian compound versus the subsequent total signal is the same in all liquids. It is interesting to note that while the longer solvation components in these liquids are strongly dependent on the particular liquid, the ultrafast solvation dynamics is almost identical (within the S/N ratio of the experimental data).

However the relative amplitude of the ~400 fs component is ~0.4 for methanol and ethyl acetamide and drastically smaller in the diols (0.2, 0.15 and 0.1 in 1,2-ethanediol, 1,3-propanediol and 1,4-butanediol, respectively) and 0.2 in butylacetamide.

7.Non-Markovian model of an optically active oscillator for ultrafast solvation dynamics

1. *Systematic introduction of the optically active oscillator model: from an overdamped Brownian oscillator to a non-Markovian oscillator*

In this subsection we shall show how to obtain the various models of optically active oscillators in a systematic way.

According to the previous subsection, the solute-solvent relaxation is determined by the relaxation function $\Phi_r(t)$. Let us turn to the central magnitude $u = W_2 - W_1 - \langle W_2 - W_1 \rangle (\langle u \rangle = 0)$. The magnitude $\Phi_r(t)$ can be written for our case in the form [34]

$$\Phi_r(t) = -\frac{i}{\hbar} \lim_{\varepsilon \to +0} \int_t^\infty \langle [u, u(t)] \rangle \exp(-\varepsilon t')dt' \qquad (24)$$

where $u(t) = \exp((i/\hbar)W_1 t)\, u \exp(-(i/\hbar)W_1 t)$. If the value u consists of a sum of partial contributions $u = \sum_j u_j$, which are not correlated with each other, then the value $\Phi_r(t)$ can be represented in the form $\Phi_r(t) = \sum_j \Phi_{rj}(t)$. Here the magnitudes $\Phi_{rj}(t)$ are also determined by Eq. (24) where the value u must be substituted by u_j. The magnitudes $u_M = W_{2M} - W_{1M} - \langle W_{2M} - W_{1M} \rangle$ and u_S can serve as examples of different contributions to u. In the case of intramolecular transitions, u_j can be contributions from different optically active oscillators. For a probe solvation, the longitudinal and transverse polarizations have different contributions (see below).

It is convenient to introduce a normalized relaxation function for the j-th contribution:

$$f_{rj}(t) = \Phi_{rj}(t)/\Phi_{rj}(0) \qquad (25)$$

Let us turn to the study of $f_{rj}(t)$. Consider its Laplace-transform

$$\tilde{f}_{rj}(p) = \int_0^\infty \exp(-pt)\, f_{rj}(t)dt \qquad (26)$$

Let us construct an approximation to $f_{rj}(t)$, which is an asymptotic (long-time) series expansion (see Appendix A). Such an approach corresponds to the fitting of $f_{rj}(t)$ by two-, three- (and so on) pole formula. We shall write down the fractions obtained by this approximation for the Laplace-transform of $f_{rj}(t)$ in the form of continued fractions. For a two-pole case we have

$$\tilde{f}^{(2)}_{rj}(p) = \frac{1}{p + \dfrac{-c_{j1}}{p - (p_1+p_2)}} \qquad (27)$$

where $p_1p_2 = -c_{j1}$, c_{jn} is determined by formulae (A4) and (A5) and $-(p_1+p_2)$ is an empirical constant. The Laplace transform $\tilde{f}^{(2)}_{rj}(p)$ coincides with the Laplace transform of the BO relaxation function [17,20,23,26] for $\omega_j^2 = -c_{j1}$ and $\gamma_j = -(p_1+p_2)$, where γ_j is the attenuation of the optically active BO. Thus,the model of the optically active BO can be considered as a two-pole approximation to the relaxation function of the system under consideration, and its frequency $\omega_j = \sqrt{-c_{j1}}$. For very large attenuation $\gamma_i >> \omega_i$, $\tilde{f}_{ri}(p)$ turns to the form

$$\tilde{f}_{ri}(p) = 1/ (p + \tau_c), \qquad (28)$$

where $\tau_c = \omega_i^2/\gamma_i$, and corresponds to the Kubo's stochastic model [42].

For a three-pole case we obtain (see Appendix A):

$$\tilde{f}^{(3)}_{rj}(p) = \frac{1}{p - \dfrac{c_{j1}}{p + \dfrac{c_{j1} - c_{j2}/c_{j1}}{p - (p_1+p_2+p_3)}}} \qquad (29)$$

$\tilde{f}^{(3)}_{rj}(p)$ coincides with the Laplace transform of the relaxation function of the NMO with an exponential memory $\varphi_j(t) = \varphi_j(0)\exp(-\alpha_j|t|)$ [17,26] for $\omega_j^2 = -c_{j1}$, $\varphi_j(0) = c_{j1}-c_{j2}/c_{j1}$ and $\alpha_j = -(p_1+p_2+p_3)$ is an empirical constant . The function $\varphi_j(t)$ describes the memory effects in the relaxation process.Thus, the model of an optically active NMO with an exponential memory function $\varphi_j(t)$ can be considered as a three-pole approximation to the relaxation function of the system under consideration.

According to the results obtained in this section and Appendix A, the optically active oscillator model can be considered as the corresponding N-pole approximation to the relaxation function. The analytical forms of a classical and a quantum relaxation functions are the same, and they are distinguished only by the formulae for the coefficients c_{jn} (Eqs. (A4) or (A5)). Thus in the quantum case one does not need to determine a correct quantum correlation function for an NMO itself which is a rather complex problem.

2.*Applications of the non-Markovian oscillator model with exponential memory.*

In this subsection we shall apply the relaxation function of the NMO model with an exponential dependence of $\varphi_j(t)$, calculated in Appendix A, for the description of ultrafast solvation dynamics. Let us introduce the mean relaxation time of the ith oscillator τ_{ri} by the formula $\tau_{ri} = \int_0^\infty f_{ri}(t)dt$. It is easy to show that $\tau_{ri} = \tilde{f}_{ri}(0) = \tilde{\varphi}_i(0)/\omega_i^2 \equiv \gamma_i(0)/\omega_i^2$, where $\tilde{\varphi}_i(p)$ is the Laplace transform of the memory function $\varphi_j(t)$, and $\gamma_i(0)$ is the frequency dependent attenuation $\gamma_i(\omega)$ for $\omega = 0$. For an ensemble of oscillators $\tau_r = \sum_i m_i\tau_{ri}$ where $m_i = \Phi_{ri}(0)/\sum_j \Phi_{rj}(0)$ is the normalized weight of oscillator i.

For the underdamped regime of the NMO model with an exponential dependence of $\varphi_i(t)$ we obtain (see Appendix A)

$$f_{ri}(t) = \frac{a^2+w^2}{(3a+1)^2+w^2}\left\{(2a+1)\exp(aT)\left[(1+d)\cos wT - \frac{a}{w}(3+d)\sin wT\right] - 2a\exp\left[-(2a+1)T\right]\right\} \quad (30)$$

where $a \pm iw$ and $-(2a+1)$ are the roots of the denominator in Eq. (A8) for the Laplace transform $\tilde{f}_{ri}(p)$, $a < 0$, $2a+1 > 0$, $T=\alpha t$, $d = (4a+1)/(a^2+w^2)$. One can see from Eq. (30) that unlike the BO, the NMO has a non-oscillating component even for the underdamped regime.

Recent experimental [4] and computer simulations [45-46] studies have shown that the subpicosecond solvation dynamics is characterized by a few components: an ultrafast Gaussian followed by slower exponentials. Let us apply the NMO model to the description of the solvation dynamics. The parameters of all NMOs used below correspond to the underdamped regime (Eq. (30)). We shall consider the classical case when the relaxation function is proportional to the (classical) correlation function. Fig.9 shows experimental data [4] (circles) of the time-resolved luminescence of LDS 750 in acetonitrile and their fitting by the model of one (dotted line) and two (solid line) NMOs. One NMO describes well both the initial (Gaussian) and the long time behavior of the experimental data, similar to Kubo's stochastic modulation theory [19] and shows an oscillation for the intermediate range. The fit by two NMOs with equal normalized weigts ($m_1=m_2=0.5$) gives excellent results. $\tau_r = 133$ fs for one NMO and $\tau_r = 113$ fs for two NMOs.

Two NMOs perfectly fit the solvation dynamics simulations for the Stockmayer

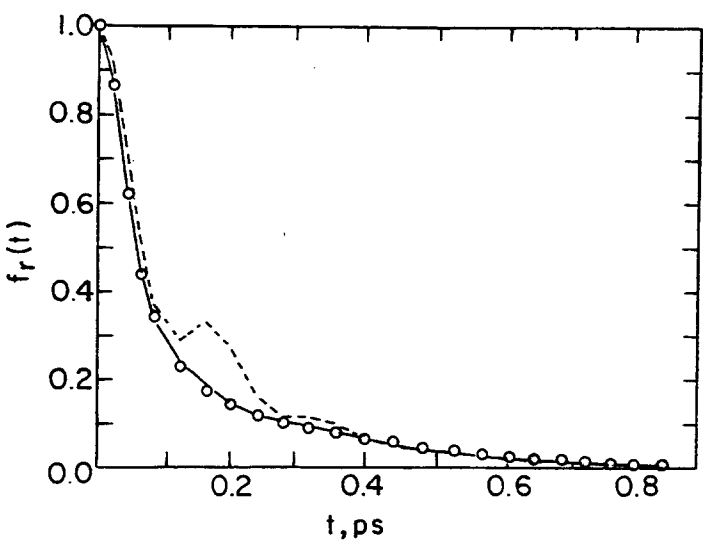

Fig. 9. Normalized relaxation (classical correlation) function of LDS 750 in acetonitrile: Circles - experiment [4]; dotted line - fitting by one NMO with two parameters: $\alpha_1 = 122$ cm^{-1} and $\gamma_1(0) = 271$ cm^{-1}, the parameter $\omega_1 = 104$ cm^{-1} is determined from the bandwidth of the initial Gaussian behavior of $f_r(t)$; solid line - fitting by two NMOs: $\omega_1 = 189$ cm^{-1}, $\alpha_1 = 913$ cm^{-1}, $\gamma_1(0) = 204$ cm^{-1}, $\omega_2 = 53$ cm^{-1}, $\alpha_2 = 115$ cm^{-1}, $\gamma_2(0) = 104$ cm^{-1}.

solvent [45] (Fig. 10; τ_r = 468 fs) and for water [24] (Fig. 11; τ_r = 128 fs). The

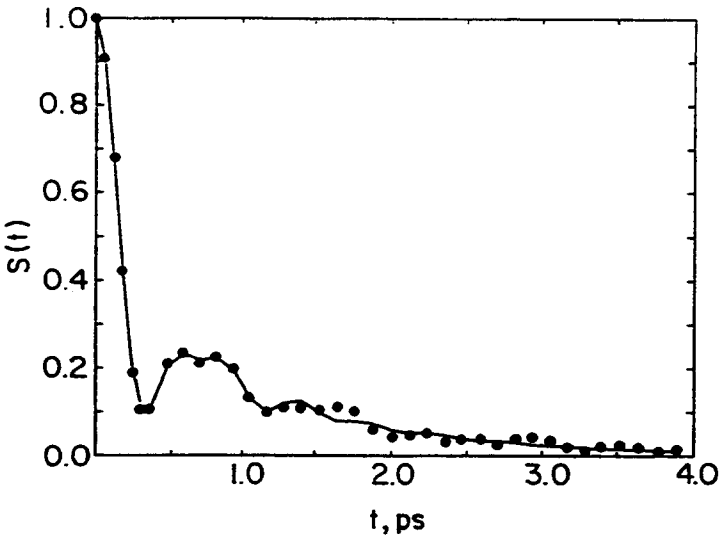

Fig. 10. Normalized correlation function S(t) for the solvation dynamics in Stockmayer solvent: Circles - simulation data [45]; solid line - fitting by two NMOs with equal normalized weights: ω_1 = 35 cm^{-1}, α_1 = 25 cm^{-1}, $\gamma_1(0)$ = 199 cm^{-1}, ω_2 = 47 cm^{-1}, α_2 =542 cm^{-1}, $\gamma_2(0)$ = 31 cm^{-1}.

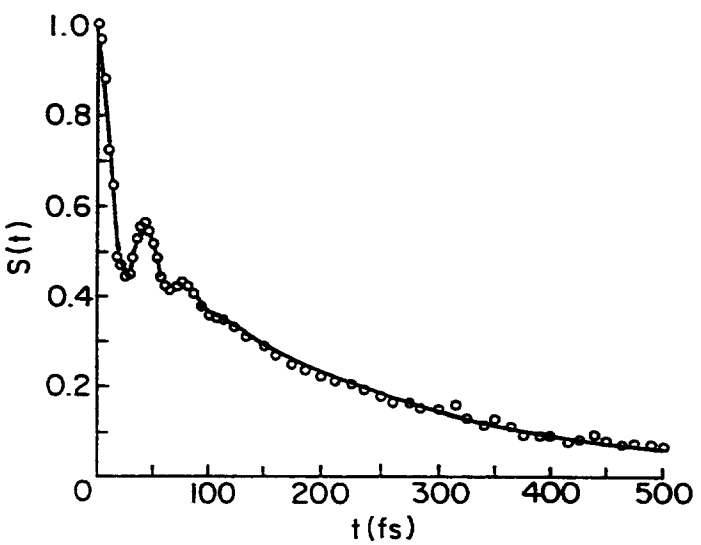

Fig. 11. Normalized correlation function S(t) for the solute in water. Circles - simulation data [24]; solid line - fit by two NMOs: ω_1 = 646 cm^{-1}, α_1 = 484 cm^{-1}, $\gamma_1(0)$ = 16235 cm^{-1}, ω_2 = 596 cm^{-1}, α_2 =790 cm^{-1}, $\gamma_2(0)$ = 606 cm^{-1}, m_1/m_2 = 3/2.

authors of [24] fit their microscopic semiclassical simulations by six BOs. The last example illustrates the strength of the NMO model with an exponential "memory" $\varphi(t)$. Two such NMOs simulate the data instead of six BOs. Correspondingly, the number of the fitting parameters reduces to 7 for the NMO model instead of 17 for the BO model. It can be understood, since the NMO with an exponential memory corresponds to a higher order approximation to the real dependence of $f_r(t)$, than BO (see above).

Thus, the NMO with exponential attenuation of the memory function is rather simple, and is an exactly soluble model for the optical response. The model of two such oscillators perfectly fits various experimental and computer simulations data on ultrafast solvation dynamics.

3. Application to Solvation Dynamics. Elucidation of the Physical Nature.

Let us consider the correlation function for the solvation dynamics process of a probe molecule in a dipole solvent. The interaction energy between a solute in electronic state **n** and the nuclear degrees of freedom of a solvent is given by the formula

$$\bar{W}_{ns} = - \int d\mathbf{r}\ \mathbf{p}(\mathbf{r})\ \mathbf{E}^{(n)}(\mathbf{r}) \tag{31}$$

where $\mathbf{p}(\mathbf{r})$ is the nuclear part of the polarization operator of the solvent, $\mathbf{E}^{(n)}(\mathbf{r})$ is the electric field created by the solute molecule in electronic state n.

Let us determine the spatial Fourier transforms of $\mathbf{p}(\mathbf{r})$ and $\mathbf{E}^{(n)}(\mathbf{r})$:

$$\mathbf{p}_{\mathbf{k}} = \int d\mathbf{r} \exp(i\mathbf{k}\mathbf{r})\mathbf{p}(\mathbf{r}), \quad \mathbf{E}^{(n)}(\mathbf{k}) = \int d\mathbf{r} \exp(i\mathbf{k}\mathbf{r})\mathbf{E}^{(n)}(\mathbf{r}) \tag{32}$$

Then we can express $\bar{W}_{ns}$ by $\mathbf{p}_{\mathbf{k}}$ and $\mathbf{E}^{(n)}(\mathbf{k})$:

$$\bar{W}_{ns} = -(2\pi)^{-3} \int d\mathbf{k}\ \mathbf{p}_{\mathbf{k}}\ \mathbf{E}^{(n)}(-\mathbf{k}) \tag{33}$$

For isotropic media the latter can be represented as a sum of the longitudinal (L) and the transverse (T) parts:

$$\bar{W}_{ns} = -(2\pi)^{-3} \int d\mathbf{k}\ \left[\mathbf{p}_{L\mathbf{k}} \mathbf{E}_L^{(n)}(-\mathbf{k}) + \mathbf{p}_{T\mathbf{k}} \mathbf{E}_T^{(n)}(-\mathbf{k})\right] \tag{34}$$

where the longitudinal components $\mathbf{p}_{L\mathbf{k}}$ and $\mathbf{E}_L^{(n)}(-\mathbf{k})$ are parallel to the vector **k**, and the transverse ones $\mathbf{p}_{T\mathbf{k}}$ and $\mathbf{E}_T^{(n)}(-\mathbf{k})$ are perpendicular to **k**. Apparently, $\mathbf{p}_{L\mathbf{k}}$ and $\mathbf{E}_L^{(n)}(-\mathbf{k})$ are uncoupled from $\mathbf{p}_{T\mathbf{k}}$ and $\mathbf{E}_T^{(n)}(-\mathbf{k})$.

For the magnitude u_s we obtain

$$u_s = W_{2s} - W_{1s} = (2\pi)^{-3} \sum_{j=L,T} \int d\mathbf{k}\ \mathbf{p}_{j\mathbf{k}} \mathbf{E}_{j12}(-\mathbf{k}) \tag{35}$$

where $\mathbf{E}_{j12}(-\mathbf{k}) \equiv \mathbf{E}_j^{(1)}(-\mathbf{k}) - \mathbf{E}_j^{(2)}(-\mathbf{k})$.

We shall calculate the correlation function $K_s(t) = \langle u_s(0)u_s(t)\rangle - \langle u_s^2\rangle$ to second order in the solvent-solute interaction [19,27]:

$$K_s(t) = \mathrm{Tr}\left[u_s \exp\left(\frac{i}{\hbar} W_{SO} t\right) u_s \exp\left(-(\beta + \frac{i}{\hbar} t)W_{SO}\right)\right] / \mathrm{Tr} \exp(-\beta W_{SO}) \tag{36}$$

Using Eqs. (35) and (36), we obtain that $K_s(t)$ consists of two contributions: $K_s(t) = K_{sL}(t) + K_{sT}(t)$. The normalized correlation function for the j-th contribution (j = L,T) is given by the formula

$$S_j(t) \equiv K_{sj}(t)/K_{sj}(0) = \int d\mathbf{k}\ |\mathbf{E}_{j12}(\mathbf{k})|^2\ C_j(\mathbf{k},t) / \int d\mathbf{k}\ |\mathbf{E}_{j12}(\mathbf{k})|^2\ C_j(\mathbf{k},0) \tag{37}$$

where

$$C_j(\mathbf{k},t) = \mathrm{Tr}\,[p_{j,-\mathbf{k}}\, p_{j\mathbf{k}}(t)\exp(-\beta W_{SO})]/\mathrm{Tr}\,\exp(-\beta W_{SO}) \qquad (38)$$

is the longitudinal (j=L) or the transverse (j=T) polarization correlation function, and

$$p_{j\mathbf{k}}(t) = \exp\left(\frac{i}{\hbar} W_{SO} t\right) p_{j\mathbf{k}} \exp\left(-\frac{i}{\hbar} W_{SO} t\right).$$

We can express the Laplace transform of $S_j(t)$ by the dielectric function of a solvent(see Appendix B):

$$\tilde{S}_L(p) = \frac{1}{p}\,\frac{\int d\mathbf{k}\,|E_{L12}(\mathbf{k})|^2\,[\varepsilon_L^{-1}(\mathbf{k},\ p) - \varepsilon_L^{-1}(\mathbf{k},\ 0)]}{\int d\mathbf{k}\,|E_{L12}(\mathbf{k})|^2\,[\varepsilon_L^{-1}(\mathbf{k},\infty) - \varepsilon_L^{-1}(\mathbf{k},\ 0)]} \qquad (39)$$

and

$$\tilde{S}_T(p) = \frac{1}{p}\,\frac{\int d\mathbf{k}\,|E_{T12}(\mathbf{k})|^2\,[\varepsilon_T(\mathbf{k},0) - \varepsilon_T(\mathbf{k},p)]}{\int d\mathbf{k}\,|E_{T12}(\mathbf{k})|^2\,[\varepsilon_T(\mathbf{k},0) - \varepsilon_T(\mathbf{k},\infty)]} \qquad (40)$$

$$\tilde{S}_j(p) = \int_0^\infty \exp(-pt)\, S_j(t)dt.$$

Apparently, $S_j(t)$ coincides with the normalized relaxation function $f_{rj}(t)$ for the classical (high temperature) case which we consider. Thus, formulae (39) and (40) express the Laplace transforms $\tilde{f}_{rL}(p) = \tilde{S}_L(p)$ and $\tilde{f}_{rT}(p) = \tilde{S}_T(p)$ by the dielectric function of a solvent.

The fact that there are two contributions to the relaxation (or correlation) function (the longitudinal (L) and the transverse (T) ones) is the basis for modelling it by two (or more) different oscillators. It is worth noting, that for dipole solvation both the L and the T contributes [49]. In the case of ion solvation, only the L contributes [27,49].

Let us consider the long wavelength polarization fluctuation as it is the fastest mode that contributes to solvation dynamics [50]. In this approximation $\varepsilon_{L,T}(\mathbf{k},p) \approx \varepsilon_{L,T}(0,p) = \varepsilon(p)$, since $\varepsilon_T(\mathbf{k}=0,\omega) = \varepsilon_L(\mathbf{k}=0,\omega)$ [54], and the Laplace transform $\tilde{S}_L(p)$ is given by the following relation:

$$\tilde{S}_L(p) = \frac{1}{p}\,\frac{\varepsilon^{-1}(p) - \varepsilon^{-1}(0)}{\varepsilon^{-1}(\infty) - \varepsilon^{-1}(0)} \qquad (41)$$

The Laplace transform of the time expansion (A3) can be written in the form [44]:

$$\tilde{f}_{rj}(p) = \frac{1}{p} + \sum_{n=1}^{\infty} c_{jn}\,/p^{2n+1} \qquad (42)$$

which can be considered as the Laurent-series expansion of $\tilde{f}_{rj}(p)$ about p = 0. The coefficients of this expansion are related to $\tilde{f}_{rj}(p)$ by the formula:

$c_{jn} = (2\pi i)^{-1} \oint p^{2n}\, \tilde{f}_{rj}(p)\, dp$, where the integration is over concentric circle centered at p = 0.

Using the expression of $\tilde{f}_{rL}(p) = \tilde{S}_L(p)$ by the dielectric function of the solvent (41), we obtain

$$c_{Ln} = c_{Tn} = (2\pi i)^{-1} \oint p^{2n-1} \frac{\varepsilon^{-1}(p) - \varepsilon^{-1}(0)}{\varepsilon^{-1}(\infty) - \varepsilon^{-1}(0)} dp \qquad (43)$$

Eq. (43) plays an important role in the model of an optically active NMO, since it relates the parameters of a NMO to an experimentally measurable magnitude: the dielectric function of a solvent.

In the general case ($\mathbf{k} \neq 0$), one must know the polarization correlation function $C_j(\mathbf{k},t)$ for the calculation of $S_j(t)$ (or $f_{rj}(t)$) (Eq. (38)). In principle, we can represent the Laplace transformation of the normalized function $C_j(\mathbf{k},t)/C_j(\mathbf{k},0)$ in the continued fraction form similar to the representation of $f_{rj}(p)$ in subsection 1. In the latter case, the coefficients c_{jn} (Eq. (A4)) depend on $\mathbf{k}$. However, a simple analytical form of the NMO model is lost for $\mathbf{k}$-dependent coefficients c_{jn}.

In this context the following question arises. Suppose, we use the NMO model with coefficients c_{jn} which does not depend on $\mathbf{k}$ (for example, with an exponential memory, used in subsection 2). Do the fitting parameters of this NMO have a physical meaning? In order to answer this question, we shall compare our NMO model with the results of the molecular hydrodynamic theory (MHT) [48,50] which have been compared [50] with the computer simulations [45].

The longitudinal correlation function $C_L(\mathbf{k},t)$ can be related to the wave vector dependent longitudinal polarization $P_L^{MHT}(\mathbf{k},t)$ calculated in Refs. 48 and 50 (see APPENDIX C):

$$\frac{P_L^{MHT}(\mathbf{k},t)}{P_L^{MHT}(\mathbf{k},0)} = \frac{C_L(\mathbf{k},t)}{C_L(\mathbf{k},0)} \qquad (44)$$

i.e., the normalized correlation function $C_L(\mathbf{k},t)/C_L(\mathbf{k},0)$ is determined by the normalized polarization $P_L^{MHT}(\mathbf{k},t)/P_L^{MHT}(\mathbf{k},0)$. For an ion solvation the Laplace-transformation of $P_L^{MHT}(\mathbf{k},t)$ is determined by [50]:

$$\frac{\tilde{P}_L^{MHT}(\mathbf{k},p)}{P_L^{MHT}(\mathbf{k},0)} = \left[p + \frac{2f_L(k)/\tau_I^2}{p + \xi_R(p)} + \frac{\bar{p}_1 k^2 \sigma^2 f_L(k)/\tau_I^2}{p + \xi_T(p)} \right]^{-1} \qquad (45)$$

where $\xi_{R,T}(p)$ are the Laplace transformations of the time dependent rotational (R) and translational (T) friction, correspondingly; σ is the solvent molecular diameter; $\bar{p}_1$ is the translational parameter which accounts for the relative importance of translational and rotational motions of the solvent; $\tau_I = (I/k_B T)^{1/2}$, I is the moment of inertia of the solvent molecules. The function $f_L(k)$ is given by

$$f_L(k) = 1-(\rho_0/4\pi)\, C(110;k)$$

where ρ_0 is the equilibrium number density of the solvent, C(110;k) is the (110) component of the spherical expansion of the wave vector and orientation dependent number density.

Using Eqs. (27),(29), (37) and (44)-(45), one can see that in the long wave length limit ($\mathbf{k} \to 0$), the right hand side of Eq. (45) has the form of the Laplace transformation of the relaxation function $\tilde{f}_{rl}(p)$ for an NMO, if

$2f_L(0)/\tau_1^2 = \omega_j^2 = -c_{j1}$.

The short time behavior of the solvation dynamics is determined by the long wave length polarization fluctuation [50] and has the following form: ~ $\exp\left\{-\frac{1}{2}\left[2f_L(0)/\tau_1^2\right]t^2\right\}$. The magnitudes in this exponent have been calculated [50] for the Stockmayer solvent model [45]. According to these evaluations, $\left[2f_L(0)/\tau_1^2\right]^{1/2} = 41.6$ cm^{-1}.

Let us compare the last value with the fitting parameters of our model consisting of two NMOs. Its short time behavior is determined by ~ $1 - \frac{1}{2}(m_1\omega_1^2 + m_1\omega_2^2)\,t^2 + \ldots \approx$ $\exp\left[-\frac{1}{2}(m_1\omega_1^2 + m_1\omega_2^2)\,t^2\right]$. Using $m_1 = m_2 = 1/2$, $\omega_1 = 35$ cm^{-1} and $\omega_2 = 47$ cm^{-1}, we obtain that $(m_1\omega_1^2 + m_1\omega_2^2)^{1/2} = 41.4$ cm^{-1}. Thus, our fitting frequencies ω_1 and ω_2 agree with the value of the parameter $f_L(0)/\tau_1^2$ which determines the orientational motion in the Stockmayer liquid.

Furthermore, Bagchi and Chandra have evaluated [50] the Einstein frequency Ω_0 for the translation motion of the solvent which determines the initial decay of the velocity correlation function. According to their calculations, $\Omega_0 = 35.5$ cm^{-1} for the system under consideration [45]. This value is very close to the frequency $\omega_1 = 35$ cm^{-1} of one of the NMOs.

Taking into account the translation motion of the solute ion itself, it is possible to obtain the following evaluation for the Einstein frequency of the solute [50]:

$$\Omega_M = \Omega_0 \sqrt{m/M} \qquad (46)$$

where m and M are the masses of the solvent molecule and the solute ion, respectively. The ratio m/M is equal to 2 for the model used in Ref.45. Using this value and the evaluation $\Omega_0 = 35.5$ cm^{-1}, we obtain from Eq.(46) $\Omega_M \approx 50$ cm^{-1}. The last value is close to the frequency $\omega_2 = 47$ cm^{-1} of the second NMO.

Thus, the fitting frequencies of our model correspond to the frequencies of the real motions in the solvation model used in Ref.45. There is only one (L) contribution to the relaxation (correlation) function of model [45] due to the ion character of the solvation. Using two NMOs in our fitting model, is the payment for the local character of the model (k=0) and/or the assumption of the exponential memory of a NMO.

There are both the longitudinal and the transverse contributions to the correlation function in simulations [24] of a probe dipole solvation in water due to the dipole character of the solvation process. In principle, it can be the justification for modelling the correlation function by two NMOs. Furthermore, in classical simulations of water, the rotational librations have a peak around 550-600 cm^{-1} [53]. The fitting frequencies of both NMOs (see Fig.11) are close to this value ($\omega_1 = 646$ cm^{-1} and $\omega_2 = 596$ cm^{-1}).

Thus, according to this discussion, the model, consisting of two NMOs with the exponential memory, reflects real motions which occur in solvation dynamics of a solute molecule.

8.Summary

In this work we have developed theoretically and experimentally the principles of a spectroscopical method based on resonance transient population gratings for a quantitative description of solvation dynamics of large molecules in liquid solutions.

We have adduced new experimental data concerning the solvation dynamics of LDS 750 in N - monosubstituted amides - ethylacetamide and butylacetamide. For a better comparison of theory and experiment we have included in our model a non-mirror-symmetry absorption and luminescence spectra of the molecule LDS 750.

We have constructed unified theoretical basis for previous empirical models of an optically active oscillator. The conception of our approach differs from other approaches. We consider the relaxation function and construct its asymptotic (long-time) series expansion that corresponds to the fit of the relaxation function by two-, three- (and so on) pole formula. As a first approximation we obtain a formula that corresponds to a classical BO model, as a second approximation - a formula that corresponds to the classical NMO model with the exponential memory, and so on. In this way, we have obtained an important conclusion that the optically active oscillator model can be considered as the corresponding N-pole approximation to the relaxation function.

In our systematic approach, the parameters of a NMO oscillator are not empiric values and can be calculated. In the long wavelength approximation ($\mathbf{k} = 0$), we have connected them with an experimentally measurable magnitude: the dielectric function of a solvent (Eqs.(27), (29), (43)).

In the general case ($\mathbf{k} \neq 0$, nonlocal approximation), the parameters of an optically active NMO are functions of $\mathbf{k}$. However, a simple analytical form for the relaxation function of a NMO is lost for $\mathbf{k}$-dependent parameters. In order to preseve the simple analytical dependence, we consider parameters of a NMO oscillator as $\mathbf{k}$-independent. In this case the NMO model becomes a semiempirical one. Nevertheless, using the simple NMO model with an exponential attenuation of the memory function for the fit of molecular dynamics computer simulations of a Stockmayer liquid [45], gives real values for the frequencies of motions occurring on ultrafast solvation dynamics (see the end of the section 7.3).

APPENDIX A

In this Appendix we shall construct an approach to $f_{rj}(t)$. Suppose that $\tilde{f}_{rj}(p)$ has only simple poles p_m. Then the function $f_{rj}(t)$ can be represented in the form [40]

$$f_{rj}(t) = \sum_m d_m \exp(p_m t) \tag{A1}$$

where d_m are the residues of the function $\tilde{f}_{rj}(p)$ at $p=p_m$. d_m are the coefficients at $(p-p_m)^{-1}$ in the Laurent-series expansion of $\tilde{f}_{rj}(p)$. The Laplace-transformation $\tilde{f}_{rj}(p)$ can be represented as

$$\tilde{f}_{rj}(p) = \sum_m d_m (p-p_m)^{-1} \tag{A2}$$

Let us turn to the calculation of the preexponential factors in Eq. (A1) for $f_{rj}(t)$. Using Eqs. (24)-(25), we shall obtain the power series expansion of $f_{rj}(t)$ in t. Such an expansion will content only even powers of t due to the evenness of $\Phi_{rj}(t)$ [34] $\left(\Phi_{rj}(t) = \Phi_{rj}(-t)\right)$:

$$f_{rj}(t) = 1 + \sum_{n=1}^{\infty} c_{jn} \frac{t^{2n}}{(2n)!} \tag{A3}$$

where $c_{jn} = -\frac{2}{\hbar \Phi_{rj}(0)} \quad \mathrm{Im} \langle u_j(0) u_j^{(2n-1)}(0) \rangle,$ (A4)

$$u_j^{(2n-1)}(0) \equiv \frac{d^{2n-1}}{dt^{2n-1}} u_j(t) \Big|_{t=0}$$

For high-temperature (classical) case

$$c_{jn} = (-1)^n \langle u_j^{(n)}(0) u_j^{(n)}(0) \rangle / \langle u_j^2(0) \rangle \qquad (A5)$$

where we used the relation $\langle u_j^{(2n)}(0) u_j^{(0)}(0) \rangle = (-1)^n \langle u_j^{(n)}(0) u_j^{(n)}(0) \rangle$.

For the classical case the expansion (A3) with coefficients (A5) coincides with the corresponding expansion of the classical correlation function [41] due to the relation $\Phi_{rj}^{cl}(t) = \beta \langle u_j(0) u_j(t) \rangle$.

Comparing Eqs. (A1) and (A3), we obtain that the coefficients c_{jn} must satisfy to the relation:

$$c_{jn} = \sum_m d_m p_m^{2n} \qquad (A6)$$

and

$$\text{a)} \quad \sum_m d_m = 1 \qquad \text{b)} \quad \sum_m d_m p_m^{2n-1} = 0 \qquad (A7)$$

Let us construct some approximation to $f_{rj}(t)$, taking into account successively two (N=2), three (N=3) (and so on) terms in the right hand of Eq. (A2). Such an approach corresponds to the fitting of $f_{rj}(t)$ by two-, three- (and so on) pole formula. Apparently, such an approach has a character of the asymptotic (long-time) series expansion of $f_{rj}(t)$ [40].

We shall write down the fractions obtained by such a way, in the form of continued fractions. Their terms can be calculated by formulae (A6)-(A7), besides the last one, which will be an empirical constant. For N = 2 we have formula (27) and For N=3 we obtain formula (29). Formulae (26) and (27) can also be obtained in the framework of a continued-fraction representation of the time correlation functions, obtained by Mori by the projection operator formalism [41,43]. Our method is simpler, and therefore we hope that our derivation will be understandable for a broader audience.

Let us calculate the relaxation function of the NMO with an exponential "memory" corresponding to three-pole approximation. Passing to dimensionless variables $s = p/\alpha$, $q = \gamma(0)\tau_r$, and $z = \alpha\tau_r$, we obtain from Eq.(29):

$$\tilde{f}_{ri}(p) = \frac{1}{\alpha} \frac{s^2+s+q/z}{s^3+ s^2+ (q/z)(1+z^{-1})s+q/z^2} \qquad (A8)$$

Here we have omitted the subscript "i" at α, s, q, z, $\gamma(0)$ and τ_r for brevity. Computing the inverse Laplace transformation of Eq.(A8), we obtain $f_{ri}(t)$.

The character of the relaxation function $f_{ri}(t)$ is determined by the roots of the polynomials in the denominator in the right-hand side of Eq.(A8). Using the properties of a cubic equation [44] , one can show that this polynomial has one real root and two conjugated roots, three real roots of which at least two are equal, or three different real roots, if the quantity $Q = (q-q_1)(q-q_2)$ is positive, zero, or negative respectively. Here

$$q_{1,2} = \frac{z^2}{8(z+1)^3} \left[(z^2+20z-8) \pm z^{1/2} (z-8)^{3/2} \right] \qquad (A9)$$

Correspondingly for Q > 0 (underdamped regime) we obtain Eq.(30).

APPENDIX B

In this Appendix we shall express the Laplace transform of $S_j(t)$ by the dielectric function of a solvent. According to the linear response theory [47,48], for the classical (high-temperature) case the following relations are held:

$$\varepsilon_L^{-1}(\mathbf{k},\omega)-1 = \frac{4\pi\beta}{V}\int_0^\infty dt\ \exp(i\omega t)\ \frac{dC_L^{tot}(\mathbf{k},t)}{dt} \tag{B1}$$

$$1-\varepsilon_T(\mathbf{k},\omega) = \frac{4\pi\beta}{V}\int_0^\infty dt\ \exp(i\omega t)\ \frac{dC_T^{tot}(\mathbf{k},t)}{dt} \tag{B2}$$

where $\varepsilon_{L,T}(\mathbf{k},\omega)$ are the dielectric functions, V is the total volume of the system and C_j^{tot} is the correlation function of the total polarization operator which is the sum of the nuclear contribution $\mathbf{p}$ and the electronic one $\mathbf{p}^{el}$. If we neglect correlations between $\mathbf{p}$ and $\mathbf{p}^{el}$ [27], C_j^{tot} can be partitioned into a nuclear part C_j and the electronic one C_j^{el}. By subtracting C_j^{el} from C_j^{tot}, one can relate C_j to a corresponding dielectric function

$$\varepsilon_L^{-1}(\mathbf{k},\omega) - \varepsilon_L^{-1}(\mathbf{k},\infty) = \frac{4\pi\beta}{V}\int_0^\infty dt\ \exp(i\omega t)\ \frac{dC_L(\mathbf{k},t)}{dt} \tag{B3}$$

$$\varepsilon_T(\mathbf{k},\infty) - \varepsilon_T(\mathbf{k},\omega) = \frac{4\pi\beta}{V}\int_0^\infty dt\ \exp(i\omega t)\ \frac{dC_T(\mathbf{k},t)}{dt} \tag{B4}$$

where $\varepsilon_j(\mathbf{k},\infty)$ represents the limit of $\varepsilon_j(\mathbf{k},\omega)$ for optical frequencies.

One can consider the right hand sides of Eqs. (B3) and (B4) as the the Laplace transform of functions $\frac{4\pi\beta}{V}\ \frac{dC_j(\mathbf{k},t)}{dt}$ for the Laplace variable $p = -i\omega$. We obtain:

$$\frac{V}{4\pi\beta}\left[\varepsilon_L^{-1}(\mathbf{k},p) - \varepsilon_L^{-1}(\mathbf{k},\infty)\right] = p\tilde{C}_L(\mathbf{k},p) - C_L(\mathbf{k},0) \tag{B5}$$

$$\frac{V}{4\pi\beta}\left[\varepsilon_T(\mathbf{k},\infty) - \varepsilon_T(\mathbf{k},p)\right] = p\tilde{C}_T(\mathbf{k},p) - C_T(\mathbf{k},0) \tag{B6}$$

where $\tilde{C}_j(\mathbf{k},p) = \int_0^\infty dt\ \exp(-pt)\ C_j(\mathbf{k},t)$

and

$$C_L(\mathbf{k},0) = \frac{V}{4\pi\beta}\left[\varepsilon_L^{-1}(\mathbf{k},\infty) - \varepsilon_L^{-1}(\mathbf{k},0)\right]$$

$$C_T(\mathbf{k},0) = \frac{V}{4\pi\beta}\left[\varepsilon_T(\mathbf{k},0) - \varepsilon_T(\mathbf{k},\infty)\right]$$

Using Eqs. (37), (B5)-(B6), we can express the Laplace transform of $S_j(t)$ by the dielectric function of a solvent (Eqs.(39) and (40)).

APPENDIX C

Let us relate the longitudinal correlation function $C_L(\mathbf{k},t)$ to the wave vector dependent longitudinal polarization $P_L^{MHT}(\mathbf{k},t)$. The longitudinal field $E_L^{(n)}$ in formula

(34) is the electric field that would arise from the solute molecule in electronic state $|n>$. The nuclear polarization corresponding to the solute transition between the ground and excited states is related to the field difference $\Delta E_L(\mathbf{k},p) = E_L^{(1)}(\mathbf{k},p) - E_L^{(2)}(\mathbf{k},p)$ by the polarizability tensor tensor α_L [51]:

$$\tilde{P}_L(\mathbf{k},p) = \alpha_L(\mathbf{k},p)\, \Delta E_L(\mathbf{k},p) \tag{C1}$$

where

$$\alpha_L(\mathbf{k},p) = 4\pi\left[\varepsilon_L^{-1}(\mathbf{k}, \infty) - \varepsilon_L^{-1}(\mathbf{k}, p)\right] \tag{C2}$$

Using Eqs. (C2) and (B5), we can represent $P_L(\mathbf{k},p)$ in the form:

$$\tilde{P}_L(\mathbf{k},p) = \frac{(4\pi)^2\beta}{V}\left[C_L(\mathbf{k},0) - p\tilde{C}_L(\mathbf{k},p)\right] \Delta E_L(\mathbf{k},p) \tag{C3}$$

According to the Frank-Condon principle, an electronic transition occurs instantaneously. Therefore, one can consider that the external field is switched on also instantaneously, so that [51]

$$\Delta E_L(\mathbf{k},p) = \Delta E_L(\mathbf{k})/p \tag{C4}$$

Inserting (C4) into Eq. (C3), we finally obtain

$$\tilde{P}_L(\mathbf{k},p) = \frac{(4\pi)^2\beta}{V}\left[\frac{C_L(\mathbf{k},0)}{p} - \tilde{C}_L(\mathbf{k},p)\right] \Delta E_L(\mathbf{k}) \tag{C5}$$

Computing the inverse Laplace transform of both sides of Eq. (C5), we obtain:

$$P_L(\mathbf{k},t) = P_L(\mathbf{k},\infty) - \frac{(4\pi)^2\beta}{V} C_L(\mathbf{k},t)\, \Delta E_L(\mathbf{k}) \tag{C6}$$

where

$$P_L(\mathbf{k},\infty) = \frac{(4\pi)^2\beta}{V} C_L(\mathbf{k},0)\, \Delta E_L(\mathbf{k}) \tag{C7}$$

since $C_L(\mathbf{k},\infty) = 0$ according to the properties of correlation functions.

The polarization $P_L(\mathbf{k},t)$ (Eq. (C6)) is determined in the spirit of the Born theory ofsolvation [51,52]: the charge (or the charge distribution) is instantaneously created at t=0 on a tagged particle which was in thermal equilibrium with the solvent before the external field was applied. However, the MHT considers an inverse situation: the decay of the equilibrium solvation energy after the charge of the solvated ion is turned off [50]. Therefore, the polarization $P_L(\mathbf{k},t)$ is related to the polarization calculated from the MHT by the expression:

$$P_L(\mathbf{k},t) = P_L(\mathbf{k},\infty) - P_L^{MHT}(\mathbf{k},t) \tag{C8}$$

Comparing Eqs. (C7) and (C8), we obtain Eq.(45).

References

1. M.A. Kahlow, W. Jarzeba, T.P. Du Bruil, P.F Barbara, Rev. Sci. Instrumen. **59**, 1098 (1988).
2. M. Maroncelli, G.R. Fleming. J. Chem. Phys. **89**, 875 (1988).
3. E.W. Castner, Jr, M. Maroncelli, G.R. Fleming. J. Chem. Phys. **86**, 1090 (1987).
4. S.J. Rosenthal, Xiaoliang Xie, Mei Du, G.R. Fleming. J. Chem. Phys. **95**, 4715 (1991).
5. M. Cho, S.J. Rosenthal, N.F. Scherer, L.D. Ziegler, G.R. Fleming. J. Chem. Phys. **96**, 5033 (1992).
6. D.A. Wiersma, E.T.J. Nibbering, K. Duppen, in: Ultrafast Phenomena VIII, eds. J.-L. Martin, A. Migus, G.A. Mourou, A.H. Zewail (Springer-Verlag, Berlin-Heidelberg, 1993) pp. 611-615.

7. R. Richert, S.Y. Goldberg, B. Fainberg, D. Huppert, in: Reaction Dynamics in Clusters and Condensed Phases, eds. J. Jortner, R.D. Levine, and B. Pullman (Kluwer Academic Publishers, Dordrecht, 1994) pp. 227-244.
8 B. Fainberg, R. Richert, S.Y. Goldberg, D. Huppert, Journ. Luminesc. **60-61**, 709 (1994); S.Y. Goldberg, E. Bart, A. Meltsin, B.D. Fainberg, and D. Huppert, Chem. Phys, **183**,217 (1994).
9. J.-Y. Bigot , M.T. Portella, R.W. Schoenlein, C.J. Bardeen, A. Migus and C.V. Shank. Phys. Rev. Lett., **66**, 1138 (1991).
10. T. Joo and A.C. Albrecht, Chem. Phys, **173**, 17 (1993).
11. B.D. Fainberg, Opt. Spectrosc. **68**, 305 (1990) [Opt. Spektrosk. **68**, 525 (1990)].
12. B. Fainberg, Phys. Rev. A **41**, 849 (1993).
13. B.D. Fainberg, Opt. Spectrosc. **67**, 137 (1989) [Opt. Spektrosk. **67**, 241 (1989)].
14. B.D. Fainberg, Chem. Phys. **148**, 33 (1990).
15. B.D. Fainberg, V.N. Nazarov, in: Ultrafast Phenomena in Spectroscopy, eds. E. Klose, B. Wilhelmi, Springer Proceedings in Physics, v. 49 (Springer-Verlag, Berlin, Heidelberg, 1990) pp. 305-308.
16. B. Fainberg, Israel Journ. Chemistry **33**, 225 (1993).
17. B.D. Fainberg, and D. Huppert, Nonlinear Optics (1994), in press.
18. J.T. Hynes, J. Phys. Chem. **90**, 3701 (1986).
19. I. Rips, J. Jortner, J. Chem. Phys. **87**, 2090 (1987).
20. Yu. T. Mazurenko and V.A. Smirnov, Opt. Spectrosc. **47**, 262; 360 (1979) [Opt. Spektrosk. **47**, 471; 650 (1979)].
21. T. Takagahara, E. Hanamura and R. Kubo, J. Phys. Soc. Jpn., **44**, 728 (1978).
22. B.D. Fainberg and I.B. Neporent, Opt. Spectrosc. **61**, 31 (1986) [Opt. Spektrosk. **61**,
48 (1986)]; B.D. Fainberg and I.N. Myakisheva, Soviet J. Quant. Electron. **17**, 1595 (1987) [Kvant. Elektron. **14**,2509 (1987)].
23. Y.J. Yan and S. Mukamel, J. Chem. Phys. **89**, 5160 (1988).
24. L.E. Fried, N. Bernstein and S. Mukamel, Phys. Rev. Lett., **68**, 1842 (1992).
25. E.T.J. Nibbering, K. Duppen, and D.A. Wiersma, J. Photochem. Photobiol. A: Chem. **62**, 347 (1992).
26. B.D. Fainberg, Opt. Spectrosc. **63**, 436 (1987) [Opt. Spektrosk. **63**, 738 (1987)].
27. R.F. Loring, Y.J. Yan, S. Mukamel. J. Chem. Phys. **87**, 5840 (1987).
28. M.J. Rosker, F.W. Wise, C.L. Tang, Phys. Rev. Lett., **57**, 321 (1986); F.W. Wise,M.J. Rosker, C.L. Tang, J. Chem. Phys. **86**, 2827 (1987).
29. W. Jarzeba, G.C. Walker, A.E. Johnson, M.A. Kahlow and P.F. Barbara, J. Phys. Chem. **92**, 7039 (1988).
30. V.L. Bogdanov and V.P. Klochkov. Opt. Spectrosc. **44**, 412 (1978); **45**, 51 (1978); **52**, 41 (1982) [Opt. Spektrosk. **44**, 707 (1978); **45**,95 (1978); **52**,71 (1982)].
31. B.D. Fainberg, Opt. Spectrosc. **65**, 722 (1988) [Opt. Spektrosk. **65**, 1223 (1988)].
32. Yu. T. Mazurenko, Opt. Spectrosc. **48**, 388 (1980) [Opt. Spektrosk. **48**, 704 (1980)].
33. G. Cramer. Mathematical Methods of Statistics (Princeton, U.P., N.J., 1946).
34. R. Kubo, J. Phys. Soc. Jpn., **12**, 570 (1957).
35. Yu. T. Mazurenko, V.A. Smirnov, Opt. Spectrosc. **45**, 12 (1978) [Opt. Spektrosk. **45**, 23 (1979)].
36. S.J.Bass, W.I.Nathan, R.M.Meighan, and R.H.Cole, J.Phys.Chem., **68**,509 (1964).
37. W.Danhauser and G.P.Johari, Canadian Journ. Chem., **46**, 3143 (1968).
38. G.R.Leader and J.F.Gormley, J.Am.Chem.Soc. **73**, 5731 (1951).
39. J.W.Vaughn and P.G. Sears, J.Phys.Chem. **62**, 183 (1958).
40. A. Ango, Mathematics for Electro- and Radio Engineers (Nauka, Moscow 1965) (in Russian).
41. B.J. Berne and G.D. Harp; Advan. Chem. Phys. **17** ,63 (1970).
42. R. Kubo, in "Fluctuation, Relaxation and Resonance in Magnetic Systems" D. ter Haar, ed. (Oliver Boyd, Edinburgh, 1962) pp.23-68.
43. H. Mori, Progr. Theor. Phys., **34**, 399 (1965).
44. G.A. Korn and T.M. Korn, Mathematical Handbook for Scientists and Engineers

(McGraw-Hill Publ. Company, N.-Y, 1968).
45. E. Neria., A. Nitzan, J. Chem. Phys. **96**, 5433 (1992).
46. L. Perera and M. Berkowitz, J. Chem. Phys. **96**, 3092 (1992).
47. E.L. Pollock and B.J. Alder, Annu. Rev. Phys. Chem., **32**, 311 (1981).
48. A. Chandra, B. Bagchi, J. Chem. Phys., **92**, 6833 (1990).
49. A. Chandra, B. Bagchi, J. Chem. Phys., **99**, 553 (1993).
50. B. Bagchi, A. Chandra, J. Chem. Phys., **97**, 5126 (1992); S. Roy, B. Bagchi, J. Chem. Phys., **99**, 1310 (1993).
51. L.E. Fried, S. Mukamel, J. Chem. Phys., **93**, 932 (1990).
52. M. Born, Z. fur Phys, **1**, 45 (1920).
53. S. Roy, B. Bagchi, J. Chem. Phys., **99**, 9938 (1993).
54. R.F. Loring, S. Mukamel. J. Chem. Phys. **87**, 1272 (1987).